

Estimation of Spectral Clustering Hyper Parameters

Sioan Zohar and Chun Hong Yoon

Photon Data and Controls Systems, Linac Coherent Light Source, SLAC National Accelerator Laboratory 2575 Sand Hill Rd, Menlo Park, CA 94025

(Dated: 11 May 2022)

Robust automation of analysis procedures capable of handling diverse data sets is critical for high data throughput experiments at the Linac Coherent Light Source (LCLS). One challenge encountered in this process is determining the number of clusters required for the execution of conventional clustering algorithms. It is demonstrated here that bi-cross validation of the inverted and regularized Laplacian used in the spectral clustering algorithm, yields a robust minimum at the predicted number of clusters and kernel hyper parameters. These results indicate that the process of estimating the number of clusters should not be divorced from the process of estimating other hyper parameters. Applying this method to LCLS x-ray scattering data demonstrates the ability to identify clusters of dropped shots without manually setting boundaries on detector fluence and provides a path towards identifying rare events.

Keywords: Suggested keywords

I. INTRODUCTION

X-Ray Free Electron Lasers (X-FELs)¹ are remarkable instruments capable of producing highly coherent x-ray pulses less than 20 fs in duration. Since their inception, X-FELs have made contributions to a diverse range of disciplines spanning from condensed matter² and atomic molecular optics³ to structural biology⁴ and femto-second chemistry⁵. The success of the Linac Coherent Light Source (LCLS) is due, in part, to the high throughput data system's⁶ ability to write to disk on a per-pulse basis. Originally developed in order to filter out low fluence shots in post processing, shot-by-shot recording has since shifted the data collection paradigm and provided researchers with the means to compensate x-ray/laser timing jitter⁷, out run x-ray damage accumulation in protein crystallography experiments^{8,9}, and offers the potential to extract new physics by identifying rare events¹⁰.

The analysis of data is one of the primary challenges preventing rapid dissemination of results; as of today, data collected at LCLS requires approximately 2.5 years of analysis before results are published. Efforts to expedite the analysis have motivated the development of a high performance computing infrastructure, user friendly abstraction layers¹¹, and novel algorithms¹². One promising avenue for streamlining data analysis is the exploitation of clustering algorithms. Such algorithms are currently used to cluster diffraction images of protein conformations collected in diffract and destroy experiments¹², but also have the potential to identify rare events¹⁰. One impediment to this approach is the problem of estimating the hyper parameters and number of clusters required for executing clustering algorithms. Early work estimating the number of clusters used a combination of gap methods¹³, distortion meth-

ods methods¹⁴, stability approaches^{15,16}, and non parametric methods¹⁷. These approaches are generally considered to be heuristic with well understood limitations and require assumptions about the cluster distribution. More recent work¹⁸ has made exciting progress in both implementing and laying the theoretical foundation for abstracting Bi-Cross Validation (BCV)¹⁹ away from its matrix formulation to estimate the number of clusters for use with the k-means algorithm. This approach¹⁸, however, requires pre-conditioning rotations to discriminate when multiple clusters are spaced along a single feature dimension. In that work¹⁸, it was predicted that applying BCV to the Laplacian matrix after the eigen-vector transformation would provide a convex surface for estimating the number of clusters.

Here, it is shown that spectral clustering hyper parameters and cluster number can be estimated by performing BCV on the inverted Laplacian matrix and finding the local minima of the resultant BCV loss function. In spectral clustering, data are embedded into a higher dimensional graph representation called the Laplacian matrix^{16,20}. The multiplicity of the Laplacian's smallest eigen-values are equal to the number of clusters. Conversely, the number of clusters is equal to the number of dominant eigen-vectors of the inverse Laplacian. BCV is a powerful method for estimating the number of dominant singular vectors needed to reconstruct the matrix without over fitting the data to the noise¹⁹. The main result is captured in equation 7 which connects the spectral clustering framework to the BCV framework. The approach proposed here implements BCV for spectral clustering without abstracting BCV away from its matrix formulation. The range where this technique succeeds and fails is explored using simulated data sets. Applying this technique to experimental LCLS x-ray scattering data separates x-ray pulses with low fluence from those with

fluence, and provides a path towards identifying clusters of rare events.

II. THEORY

Consider a set of x-ray scattering data stored within a matrix \mathbf{X} , with elements $\mathbf{X}_{i,j}$ where i and j are the rows and columns indices respectively. All entries contained within a row have been measured at the same instant, and all entries within a single column measure the same quantity. For the case of LCLS data, potential column labels are incident x-ray pulse energy, scattered pulse energy, photon energy, x-ray/laser jitter correction, or laser delay stage position. The process of clustering, in this context, means assigning labels, such as “signal of interest”, “low fluence shots”, “outliers”, or “rare events” to each of the rows.

In the spectral clustering approach, clusters are identified by applying k-means clustering on the k smallest eigen-vectors, v , of the Laplacian matrix, \mathbf{L} , where k is the number of clusters. That is,

$$\mathbf{L} = \mathbf{D} - \mathbf{W} \quad (1)$$

where \mathbf{D} is the degree matrix. The weighting \mathbf{W} matrix chosen here is calculated using the radial basis function (RBF) kernel²¹ such that

$$\mathbf{W}_{i,j} = \mathbf{W}_{j,i} = \exp \left[-\Gamma \sum_m (\mathbf{X}_{i,m} - \mathbf{X}_{j,m})^2 \right] \quad (2)$$

where i and j are the row and column indices of \mathbf{W} , and Γ is a hyper parameter that is inversely proportional to root of the expected distance between points within a cluster. In practice, the Laplacian is normalized by

$$\mathbf{L}_n = \mathbf{D}^{-1/2} \mathbf{L} \mathbf{D}^{-1/2} = \mathbf{I} - \mathbf{D}^{-1/2} \mathbf{W} \mathbf{D}^{-1/2} \quad (3)$$

where \mathbf{L}_n is the normalized Laplacian. Using these definitions, the spectral clustering method proceeds by solving the generalized eigen-vector problem

$$\mathbf{L}_n v = \lambda \mathbf{D} v, \quad (4)$$

implementing k-means on the diagonalized feature space, and propagating the resultant labels from k-means back to \mathbf{X} .

The procedure for estimating the number of clusters and Γ by performing BCV on the inverted \mathbf{L}^{-1} proceeds as follows. The Laplacian is, by construction, a singular matrix that cannot be inverted. This drawback is circumvented by add a regularization term, \mathbf{R} . That is

$$\mathbf{L}_r = \mathbf{L}_n + \xi \mathbf{R} \quad (5)$$

where ξ is a scalar regularization parameter. In this work, ξ is empirically determined to be of the order 1e-9 to 1e-14. The matrix \mathbf{R} is

$$\mathbf{R} = \mathbf{H} - \mathbf{H}^T \mathbf{L}_n \mathbf{H} \quad (6)$$

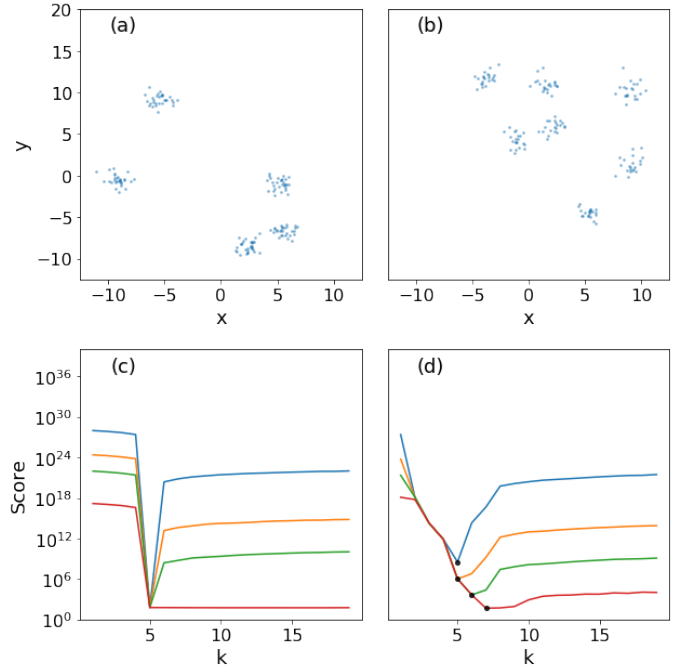


FIG. 1 (a) A set of 150 samples occupying a 7D feature space are clustered into 5 groups and projected onto 2D. (b) The inter-cluster spacing is reduced by reducing the feature space from 7D to 2D and increasing the number of clusters from 5 to 7. (c) The BCV score dependence on the number of clusters for regularization parameter values of 1e-14 (blue), 6.3e-13 (orange), 1e-12 (green), 2.5e-9 (red). The score minimum occurs at 5 which is the expected number of clusters. (d) When the inter-clustering spacing is reduced, BCV does not robustly estimate the number of clusters, since the score minimum (black dots) does not occur at the same k value for all values of ξ and only occurs at the expected value of 7 for $\xi = 2.5e-9$.

where \mathbf{H} is a Haar distributed random matrix²². Adding $\xi \mathbf{R}$ to \mathbf{L}_n , as opposed to adding $\xi \mathbf{H}$ directly, guarantees the resultant matrix \mathbf{L}_r can be inverted. The BCV loss function for \mathbf{L}_r^{-1} is calculated as described in¹⁹ by breaking \mathbf{L}_r^{-1} into quadrants.

$$\mathbf{L}_r^{-1} = \begin{bmatrix} \mathbf{A} & \mathbf{B} \\ \mathbf{C} & \mathbf{E} \end{bmatrix} \quad (7)$$

The bottom right quadrant has been labeled in this work \mathbf{E} , deviating from the notation in previous literature¹⁹ so as not to be confused with the degree matrix \mathbf{D} . For this work, \mathbf{A} was designated as the hold out and 2x2 BCV was configured such that the sub matrices $\mathbf{A}, \mathbf{B}, \mathbf{C}, \mathbf{D}$ have the same number of rows and columns. This sub-matrix partitioning is close to the optimal 52% holdout size for square matrices²³. The BCV loss function is

$$BCV(k, \Gamma) = \sum_{i,j} (\mathbf{A} - \mathbf{B}(\hat{\mathbf{E}}^{(k)})^+ \mathbf{C})_{i,j}^2 \quad (8)$$

where $(\hat{\mathbf{E}}^{(k)})^+$ is the Penrose pseudo inverse of $(\hat{\mathbf{E}}^{(k)})$

$$(\hat{\mathbf{E}}^{(k)})^+ = ((\hat{\mathbf{E}}^{(k)})^T \hat{\mathbf{E}}^{(k)})^{-1} (\hat{\mathbf{E}}^{(k)})^T \quad (9)$$

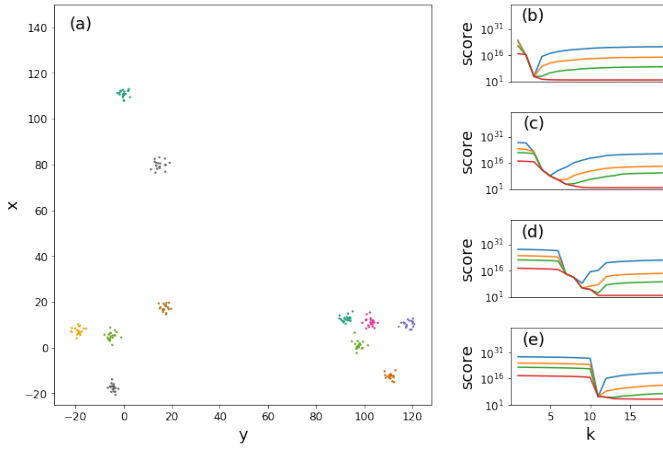


FIG. 2 Demonstration of cluster identification at different length scales. (a) a set of 150 samples clustered in to 11 groups that appears as 3 clusters on longer length scales. (b) density map of their score dependence on Γ and k . Regularization values are $1e-14$, (blue), $6.3e-13$ (orange), $1e-12$ (green), $2.5e-09$ (red). The score as function of the cluster number k is shown for Γ equal to 0.005, 0.028, 0.158 and 1.58 for panels (b), (c), (d), and (e) respectively.

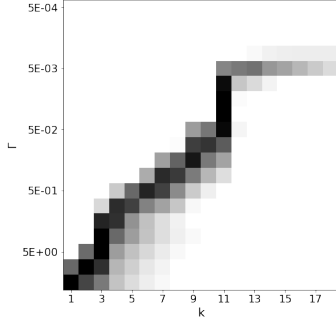


FIG. 3 Density map of the score dependence on Γ and k for $\xi = 1e-14$. The dark and light regions correspond to low and high scores respectively.

and $(\hat{\mathbf{E}}^{(k)})$ is the SVD reconstruction of \mathbf{E} using k number of basis vectors. In this work, the procedure starting from equation 7 was iterated ~ 40 times with \mathbf{L}_r^{-1} being shuffled each iteration before being decomposed into sub matrices. The BCV score used to determine the number of clusters is the average BCV score over all iterations.

III. NUMERICAL SIMULATIONS

The performance of this approach was benchmarked for a range of hyper parameters using the scikit-learn version 0.19.1, numpy version 1.14.2, and scipy version 0.19.1 packages^{24–27}. The source code used to generate the simulations can be found here²⁸, and an executable step by step walk through can be cloned from this repository²⁹.

In Figure 1 (a) a set of 5 simulated clusters projected from 7 dimension feature space onto 2 dimensions is shown. Panel (b) shows 7 simulated clusters generated in a 2D feature space. The BCV loss function minimum

was found by iterating over increasing values of cluster number, k , and length scales, Γ and calculating the BCV at each point. The BCV score's dependence on k for the clusters in panel (a) and (b) are shown in panels (c) and (d) respectively. The different color lines shown in (c) and (d) correspond to increasing values of the regularization parameter. The BCV score in (c) has a minimum at $k=5$ correctly identifying the number of clusters. This estimate is robust for changing regularization values except for large regularization, where the score minimum no longer occurs at the expected number of clusters and moves to arbitrarily large k . The inter-cluster distance for points in Fig. 1 panel (b) is decreased with respect to panel (a) by increasing the number of clusters from 5 to 7 and reducing the feature space dimension from 7 to 2. The BCV score for the points in panel (b) are shown in panel (d). For a fixed value of Γ , the cluster number estimation procedure is not robust since the score minimum does not reliably estimate the number clusters for all values of ξ .

In Figure 2 (a), a set of clusters in 2D are shown. Depending on the Gaussian kernel width chosen to construct the affinity matrix, the clusters can be partitioned into 3 or 11 different clusters. The scores plotted as a function of the number of clusters are shown in panels (b), (c), (d), and (e) for values of Γ equal to 0.005, 0.028, 0.158 and 1.58 respectively. The different colored curves are for different values of the regularization parameter ξ . For the smallest regularization values (blue curves), two global minimum occurring at Γ values of 1.58 (Fig. 2 (b)) and 0.005 (Fig. 2 (e)) occur at k equal to 3 and 11 respectively. In Figure 3 a heat map of the BCV's score value's dependence upon the gaussian kernel width and number of cluster is shown for $\xi = 10^{-14}$. The RBF parameter Γ can be converted into a characteristic length scale σ , using $\Gamma = 1/(2\sigma^2)$. The two local minimum observed at $k = 11$ and $k = 3$ have corresponding σ values of the orders of 1 and 10 respectively, which correspond to two different length scales at which the clusters can be grouped. This result is exciting because not only is k estimated, but multiple values of Γ are also estimated.

IV. EXPERIMENTAL DATA

In Figure 4 the effectiveness of this approach in identifying low fluence x-ray shots from an x-ray scattering experiment is shown. The feature space is 12 dimensions with column labels corresponding to intensity of x-rays scattered off the sample, incident intensity downstream the monochromator, 4 different incident intensity diagnostics from upstream the monochromator, laser delay stage position, laser power, arrival time monitor mean and FWHM, photon energy, and the photon energy product with the incident intensity down stream the monochromator. The energy-intensity product linearizes the chromatic non-linearity observed when the photon energy is tuned to the steep part of absorption edges³⁰.

An additional cluster density vector estimated from the diagonal of the Laplacian calculated from 7000 samples for a $\Gamma = 1e-2$ was appended to this feature space. This circumvents the heterogeneous density problem encountered in spectral clustering by including the density as part of the feature space. Clustering was performed on a total of 750 rows from this feature space. Eleven clusters are identified with populations of the dominant first three clusters containing on average 573, 62, 43 data points, with the rest of the data points be spread over the remaining clusters. This approach separates out the dominant cluster (blue histogram) which corresponds to signal of interest from the dropped shots with no fluence (orange bars). It is stressed that the last figure presented here is analyzed on less than 1 % of the entire data and does not represent the expected number of clusters if the full data set were to be used.

V. DISCUSSION

There are several advantages for using the matrix formulation¹⁹ of BCV with data embedded into a higher dimensional space, as opposed to the abstracted BCV form in the non embedded feature space¹⁸. One advantage is that the pre-conditioning rotations needed for making clusters that lie along one dimension separable are no longer required. Another advantage over is that since the matrix BCV formulation does not require a classification, the prerequisite hyper parameter estimation for the classification kernel is also not needed.

The ability to simultaneously estimate both the Γ parameter and number of clusters is not serendipitous. Intuitively, one recognizes that asking “how many clusters are present in some region” can not be separated from the question of “what length scales do the clusters appear on?”

The spectral clustering algorithm used here employed the RBF kernel to convert the adjacency matrix L^2 into the weighting matrix. This particular RBF kernel has a single scalar parameter, Γ . The approach demonstrated here to optimize Γ could be used to generalize Γ from a scalar to a covariance matrix (or more complicated kernel) with each matrix element being optimized using the BCV approach. Scanning such a hyper parameter space would require $O(e^n)$ time, where n is the number of hyper parameters. A more efficient minimum finding approach exploiting gradient descent methods would be required to reduce the time complexity. Initializing gradient descent methods at different hyper parameter values would provide a path towards avoiding the trivial solution describing a single cluster at large length scales.

Looking forward, there are several pre-requisites that would need to be met for this approach to be widely adapted. A rigorous proof of the ability to simultaneously optimize hyper parameters would have to be shown. Ideally, this proof would provide insight on how to estimate the regularization parameter. Such a proof could use eigen-vector decomposition of the inverted Laplacian, as

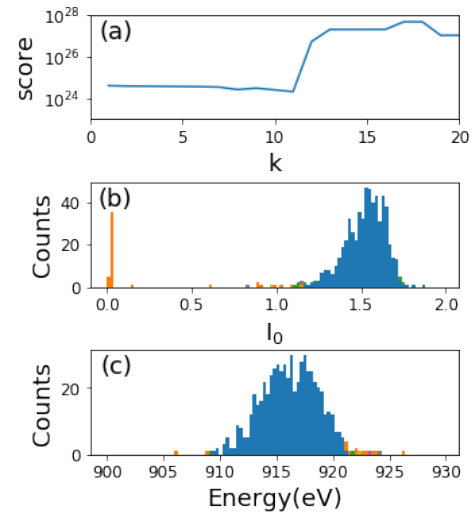


FIG. 4 (a) the BCV score minimum occurs for 11 clusters. (b) histogram the incident pulse energy measured in a gas detector upstream the monochromator. The orange and blue histogram the dropped shots and signal of interest respectively. (c) histogram of the photon energy generated upstream the monochromator.

opposed to SVD decomposition, and exploit the Laplacian matrix’s symmetry. Another challenge is that the size of the Laplacian matrix scales with number of points squared; thus typical LCLS data sets which have on the order of $3E5$ data points would require finding the SVD of a $3E5 \times 3E5$ matrix which is on the order of a terabytes and exceeds typical host machine RAM. Sparse matrix methods would be required to avoid memory overflow.

VI. CONCLUSION

In conclusion, a direct matrix implementation of BCV for estimating both the number of clusters and kernel hyper parameters required for spectral clustering has been demonstrated. This was accomplished by applying the matrix formulation for BCV directly to the inverted Laplacian matrix used in spectral clustering. The resulting BCV loss function has robust minima that occur at different cluster numbers depending upon the length scales determined by RBF kernel parameter. The results here provide a path towards generalized hyper parameter optimization for spectral clustering algorithms.

We thank Art B. Owen for providing fruitful discussions and insights. This work was performed in support of the LCLS project at SLAC supported by the U.S. Department of Energy, Office of Science, Office of Basic Energy Sciences, under Contract No. DE-AC02-76SF00515.

¹T. Ishikawa, H. Aoyagi, T. Asaka, Y. Asano, N. Azumi, T. Bizen, H. Ego, K. Fukami, T. Fukui, Y. Furukawa, *et al.*, *nature photonics* **6**, 540 (2012).

²D. J. Higley, A. H. Reid, Z. Chen, L. L. Guyader, O. Hellwig, A. A. Lutman, T. Liu, P. Shafer, T. Chase, G. L. Dakovski, *et al.*, *arXiv preprint arXiv:1902.04611* (2019).

³J. Yang, X. Zhu, T. J. Wolf, Z. Li, J. P. F. Nunes, R. Coffee, J. P. Cryan, M. Gühr, K. Hegazy, T. F. Heinz, *et al.*, *Science* **361**, 64 (2018).

- ⁴P. Nogly, T. Weinert, D. James, S. Carbajo, D. Ozerov, A. Furrer, D. Gashi, V. Borin, P. Skopintsev, K. Jaeger, *et al.*, *Science* **361**, eaat0094 (2018).
- ⁵K. Hong, H. Cho, R. W. Schoenlein, T. K. Kim, and N. Huse, *Accounts of chemical research* **48**, 2957 (2015).
- ⁶J. Thayer, D. Damiani, C. Ford, I. Gaponenko, W. Kroeger, C. O’Grady, J. Pines, T. Tookey, M. Weaver, and A. Perazzo, *Journal of Applied Crystallography* **49**, 1363 (2016).
- ⁷S. Droste, L. Shen, V. E. White, E. Diaz-Jacobo, R. Coffee, S. Zohar, A. H. Reid, F. Tavella, M. P. Minitti, J. J. Turner, *et al.*, in *CLEO: Science and Innovations* (Optical Society of America, 2019) pp. SF3I–7.
- ⁸J. C. Spence, *Structural Dynamics* **4**, 044027 (2017).
- ⁹C. Kupitz, J. L. Olmos Jr, M. Holl, L. Tremblay, K. Pande, S. Pandey, D. Oberthür, M. Hunter, M. Liang, A. Aquila, *et al.*, *Structural Dynamics* **4**, 044003 (2017).
- ¹⁰R. Schoenlein, S. Boutet, M. Minitti, and A. Dunne, *Applied Sciences* **7**, 850 (2017).
- ¹¹D. Damiani, M. Dubrovin, I. Gaponenko, W. Kroeger, T. Lane, A. Mitra, C. O’Grady, A. Salnikov, A. Sanchez-Gonzalez, D. Schneider, *et al.*, *Journal of Applied Crystallography* **49**, 672 (2016).
- ¹²C. H. Yoon, P. Schwander, C. Abergel, I. Andersson, J. Andreasson, A. Aquila, S. Bajt, M. Barthelmess, A. Barty, M. J. Bogan, *et al.*, *Optics express* **19**, 16542 (2011).
- ¹³R. Tibshirani, G. Walther, and T. Hastie, *Journal of the Royal Statistical Society: Series B (Statistical Methodology)* **63**, 411 (2001).
- ¹⁴C. A. Sugar and G. M. James, *Journal of the American Statistical Association* **98**, 750 (2003).
- ¹⁵R. Tibshirani and G. Walther, *Journal of Computational and Graphical Statistics* **14**, 511 (2005).
- ¹⁶U. Von Luxburg *et al.*, *Foundations and Trends® in Machine Learning* **2**, 235 (2010).
- ¹⁷A. Fujita, D. Y. Takahashi, and A. G. Patriota, *Computational Statistics & Data Analysis* **73**, 27 (2014).
- ¹⁸W. Fu and P. O. Perry, arXiv preprint arXiv:1702.02658 (2017).
- ¹⁹A. B. Owen, P. O. Perry, *et al.*, *The annals of applied statistics* **3**, 564 (2009).
- ²⁰U. Von Luxburg, *Statistics and computing* **17**, 395 (2007).
- ²¹K.-M. Chung, W.-C. Kao, C.-L. Sun, L.-L. Wang, and C.-J. Lin, *Neural computation* **15**, 2643 (2003).
- ²²F. Mezzadri, arXiv preprint math-ph/0609050 (2006).
- ²³P. O. Perry, arXiv preprint arXiv:0909.3052 (2009).
- ²⁴F. Pedregosa, G. Varoquaux, A. Gramfort, V. Michel, B. Thirion, O. Grisel, M. Blondel, P. Prettenhofer, R. Weiss, V. Dubourg, J. Vanderplas, A. Passos, D. Cournapeau, M. Brucher, M. Perrot, and E. Duchesnay, *Journal of Machine Learning Research* **12**, 2825 (2011).
- ²⁵T. E. Oliphant, *A guide to NumPy*, Vol. 1 (Trelgol Publishing USA, 2006).
- ²⁶T. E. Oliphant, *Computing in Science & Engineering* **9**, 10 (2007).
- ²⁷S. Van Der Walt, S. C. Colbert, and G. Varoquaux, *Computing in Science & Engineering* **13**, 22 (2011).
- ²⁸“Systematic studies spectral clustering,” https://github.com/sioan/examples_for_learning/blob/master/spectral/systematic_studies_of_spectral_clustering_sigma.ipynb (), accessed: 2019-05-7.
- ²⁹“Demonstration of bi-cross validation for determining spectral clustering parameters and cluster number,” https://github.com/sioan/bcv_spectral_clustering/blob/master/spectral_clustering.ipynb (), accessed: 2019-05-7.
- ³⁰S. Zohar and J. J. Turner, *Optics letters* **44**, 243 (2019).